PLASMA SHEATH ANALYSIS AND CURRENT CALCULATIONS FROM THE POTENTIAL DISTRIBUTION AROUND INTERBALL AURORAL PROBE

M Bouhram[1], N Dubouloz[2], M Hamelin[1], S A Grigoriev[3], and K Torkar[4]

[1]CETP-CNRS, 4 Avenue de Neptune, 94107 St-Maur Cedex, France.
Phone: +1 45 11 42 73, Fax: +1 48 89 44 33, email: mehdi.bouhram@cetp.ipsl.fr
[2]LPCE-CNRS, 45071 Orleans Cedex, France
[3]Mathematical Dept., Kaliningrad State University, 236041 Kaliningrad, Russia
[4]Space Research Institute, A.A.S, Inffeldgasse 12, A-8010 Graz, Austria

Abstract. The electric potential structure near Interball Auroral Probe (AP) and the determination of the floating spacecraft (S/C) potential are studied by means of three-dimensional simulations. Current-voltage characteristics of collected electrons and ejected photoelectrons are obtained by using a Laplace solution of the potential distribution. This solution includes a realistic geometry of Interball AP, and the effect of the ambient magnetic field and the electron temperature are taken into account. Comparisons with analytical theories of unmagnetized probes show that the effect of the complex S/C geometry is weak. Using the equilibrium of the computed currents flowing in and out the S/C, we could numerically derive a relation between the plasma density and the floating S/C potential. These results are used in addition to conjugated measurements aboard Interball AP to determine the photoemission production rate on the S/C sunlit surface. A value of 35 $\mu A\ m^{-2}$ is estimated. Ultimately, the aim of these simulations is to validate distribution functions of low energy ions measured by the Hyperboloid experiment aboard Interball AP.

1. INTRODUCTION

The Interball Auroral Probe (AP) launched in 1996, has an orbit with a high inclination, covering a wide range of altitudes between 700 and 20000 km, in the high-latitude magnetosphere. The ambient plasma conditions along this orbit are significantly variable, and the satellite becomes charged owing to the low plasma density and the photoelectrons extracted from solar radiations on the S/C sunlit surface. Statistical observations from electric field experiment aboard Interball AP showed that the S/C body potential Φ_s reaches positive values ranging from 0 to 10 V (Ref. 1). This potential prevents low-energy ions from reaching the Hyperboloid ion mass spectrometer (Ref. 2) aboard Interball AP. Ions of energies higher than Φ_s can be detected, but the analysis of their measurements requires a knowledge of Φ_s and the three-dimensional (3D) potential distribution surrounding the body.

The value of Φ_s insures the balance of currents flowing in and out the S/C body surface (Ref. 3). These currents are the currents of ejected photoelectrons I_{ph}, incident plasma electrons I_e, secondary electrons I_{se} due to incident electrons, and plasma ions I_i. For $\Phi_s>0$, $I_i<<I_e$ due to the ion to electron mass ratio, and can be totally neglected. I_{se} has to be taken into account when the S/C enters in eclipse (Ref. 4), but is however negligible in our case study, because Interball AP was always in sunlight at high latitudes. Therefore, only I_{ph} and I_e contribute to the balance.

Previously, several works (Refs. 2, 5 or 6) used S/C potential measurements from electric field double-probe experiments so as to derive the plasma density. However, these works assumed an unmagnetized medium, and a simple geometry for the S/C body. In our case study, Interball AP has a very complicated geometric structure including solar panels, booms, antennas, extending up to several meters. When Interball AP travels between 8000 and 20000 km altitude, the ambient magnetic field along the orbit ranges from 1 to 5 µT, corresponding to an electron gyroradius from 0.7 to 3.4 m for an energy about 1 eV. These values are comparable to the S/C body size, therefore the ambient magnetic field should be taken into account in the calculations.

Recently, a Laplace solution of the 3D potential distribution was computed (Ref. 7) by using a realistic geometry. In this paper, current-voltage characteristics of collected electrons $I_e(\Phi_s)$ and ejected photoelectrons $I_{ph}(\Phi_s)$ are performed, including a realistic S/C geometry and the effect of the ambient magnetic field. Furthermore, results enable to determine how the relation between the S/C floating potential Φ_s and the ambient plasma density N_e depends on the different parameters (e.g. magnetic field, photoemission, electron temperature) governing the S/C-plasma interaction. The resulting N_e-Φ_s curves are then used with simultaneous potential and density measurements from electric-field experiments in order to calculate the photoemission rate on the S/C sunlit surface.

2. MODEL

2.1 Potential distribution

The aim of this model is to perform accurate particle trajectories in a realistic electric field structure around Interball AP. Figure 1 displays the complex S/C geometry with all the following structures :

- The S/C body approximated as a cylinder
- Four solar panels in the x-y plane
- All booms and electric antennas

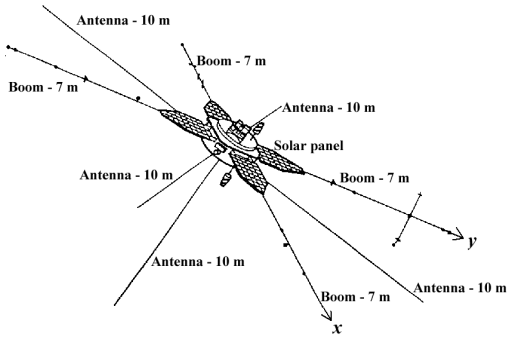

Figure 1. Geometric structure of Interball AP.

The electric potential distribution is obtained by solving the Laplace equation :

$$\partial^2\Phi/\partial x^2 + \partial^2\Phi/\partial y^2 + \partial^2\Phi/\partial z^2 = 0 \qquad (1)$$

The equation is solved by especially designed multi-grid algorithms (Ref. 7). The simulation domain Σ is rectangular with dimensions : 80×80×60 m. The S/C body is at given potential Φ_S, while the outer boundary are at a zero potential. Figure 2 shows an example of equipotential contours.

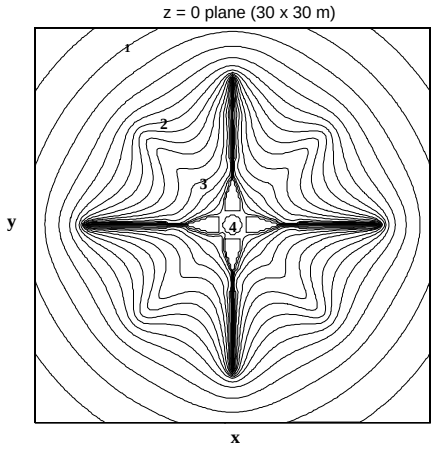

Figure 2. Equipotential contours of the potential distribution in the solar panel plane x-y. The S/C body is at + 4V.

This solution neglected the space charge density around the S/C body, as justified by the low encountered plasma densities, which imply electron Debye lengths larger than the S/C body sizes. Actually, the problem is more complicated, due to the presence of a photoelectron sheath surrounding the S/C body (Ref 8.). Numerical Particle-In-Cell simulations of photoelectron sheath in a magnetized plasma have been performed with a cylindrical satellite (Ref 9.). It was found that a Laplace solution is acceptable for first order calculations of current-voltage characteristics in the high-altitude magnetosphere. Such an approach is especially suited to S/C with a complex geometric shape, which cannot be treated by the Poisson method, due to computer capabilities.

2.2 Current calculations

We describe in this section the calculation's method of electron and photoelectron current-voltage relations from particle's trajectories. The plasma electrons are simulated by using a reservoir blanketing the simulation system Σ, and containing a drifting maxwellian electron population with a density N_e, and a temperature T_e. A fixed number of electrons is kept inside the reservoir so as maintain N_e as constant inside Σ. Two values of T_e are considered : 1 and 10 eV.

The photoelectrons are uniformly emitted from all the sunlit parts of the S/C body (solar panels and the top cylindrical surface), and are distributed in velocity according to a maxwellian distribution with a temperature T_{ph}=1.5 eV (Ref. 4) and a full emitted current density J_{ph0}. However, the determination of J_{ph0} in space conditions is not easy, as shown later.

Each particle (electron or photoelectron) is characterized by a negative charge q_e, and a mass m_e. The particle trajectories are performed by solving the equation of motion of computer particles given by :

$$m_e \, d\mathbf{V}/dt = q_e\left(\mathbf{E}(\mathbf{r}) + \mathbf{V} \times \mathbf{B_0}\right) \qquad (2)$$

where $\mathbf{B_0}$ is the ambient magnetic field and $\mathbf{E}$ is the electric field due to the S/C charging. The particles motions were advanced in each time step Δt using a leapfrog integration technique. The electric field $\mathbf{E}(\mathbf{r})$ was interpolated from the three-dimensional (3D) potential solution $\Phi(\mathbf{r})$. The magnetic field $\mathbf{B_0}$ is taken along the x-axis.

3. CURRENT-VOLTAGE CHARACTERISTICS

Particle trajectories were computed by using a Laplace solution for the 3D potential field, as described earlier. The main plasma parameters are summarized in Table 1. We performed calculations with and without magnetic field $\mathbf{B_0}$, so as to separate geometric and magnetic effects on both collected and ejected currents. Different values of $\mathbf{B_0}$ and the electron temperature T_e are considered.

Definition	Notation	Value
Spacecraft body potential	Φ_s	0-10 V
Magnetic field	B_0	0, 1, 5 μT
Electron temperature	T_e	1, 10 eV
Simulation time step	Δt	$5.7\ 10^{-8}$ s

Table 1. Summary of numerical parameters used in the simulations.

3.1 Escaping photoelectron current

The simulation for emitted photoelectrons starts at t=0 by distributing uniformly a maxwellian population on the S/C sunlit surfaces. When t>0, the motion of each computer photoelectron is followed by solving (2). Providing the photoemission rate J_{ph0} is known, it is enough to determine the fraction of photoelectrons which left the simulation system.

Figure 3 shows the resulting photoelectron current-voltage relationships, obtained by varying the ambient magnetic field. The ejected current for B_0=0 (circles) is compared to the currents ejected from a small spherical electrostatic sample or a point source (dashed line) and from a planar surface (dotted line), given by (Ref. 4):

Small sample :

$$I_{Sph} = A_S J_{ph0}\left(1 + \Phi_s / T_{ph}\right)\exp\left(-\Phi_s / T_{ph}\right) \qquad (3)$$

Planar surface :

$$I_{Pph} = A_S J_{ph0} \exp\left(-\Phi_s / T_{ph}\right) \qquad (4)$$

where A_s is the total sunlit area.

The ejected current is maximum in the point source case (body size << Debye length) and minimum in the planar surface case (body size >> Debye length), as previously reported by Grard (Ref. 4). The case of a S/C (e.g. Interball) is obviously intermediate between these two extreme cases. The ejected current-voltage characteristics for B_0=1 μT (squares) and B_0=5 μT (triangles) are smaller than the ejected currents in a unmagnetized medium. In fact, the photoelectron gyroradius is about 4.0 and 0.8 m for B_0=1 and 5 μT respectively. These values are lower than the spatial extent of Interball AP. Therefore, when $\mathbf{B_0}$ increases, a significant part of the emitted photoelectrons return to the S/C surface. Therefore, this acts as an additional process to the photoelectrons reflected by the electrostatic potential barrier effect.

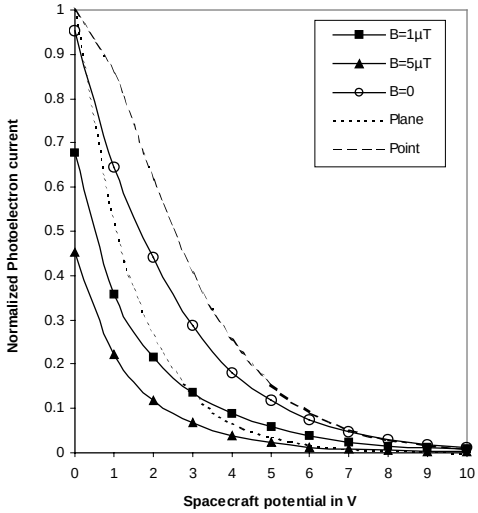

Figure 3. Current-voltage characteristics of ejected photoelectrons for different values of B_0. All currents are normalized with respect to the photoelectron saturation current.

3.2 Electron current

The simulation for plasma electrons starts at t=0 with an empty volume. When t>0, the electrons are simulated with the reservoir blanketing the volume Σ, and progressively fill the box. The collected current and the ambient density reach a quasi-steady state after approximately 70 μs. This value corresponds roughly to the average time for an electron from the reservoir to reach the S/C body across the simulation system. As shown in Table 1, electron current-voltage relationships were established by repeating simulations, for various values of the ambient magnetic field and for two electron temperatures: T_e=1 eV (solid curves) and 10 eV (dashed curves). The collected current without magnetic field (circles) is compared to the current collected by an electrostatic probe in the thick sheath limit (Ref. 3):

$$Is_e = I_{e0}\left(1+\Phi_s/T_e\right) \qquad (5)$$

where $I_{e0} = 0.026\ A_T N_e T_e^{1/2}$ denotes the electron thermal current with A_T the total area of Interball AP in m^2, N_e the plasma density in cm^{-3}, and T_e the electron temperature in eV.

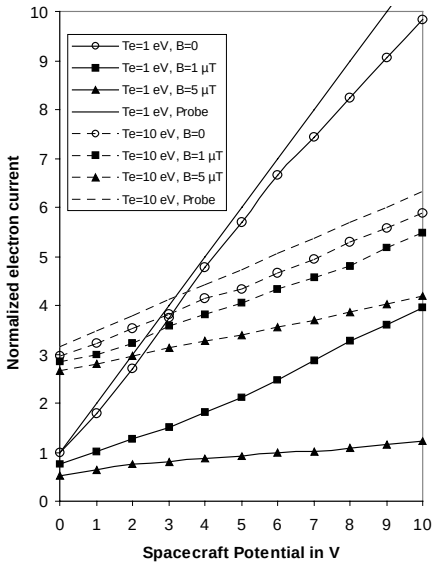

Figure 4. Current-voltage characteristics of collected plasma electrons for different values of B_0. All currents are normalized with respect to the thermal current.

The curves for B_0=0 are very close, which implies that the electron collection is not sensitive to complex geometric effects. For T_e=1 eV, the collected currents for B_0=1 µT (squares) and B_0=5 µT (triangles) are smaller than the collected current in a unmagnetized medium : the electrons collected by the body come from a bunch of field lines aligned with the magnetic shadow of the body, the transverse size depending mainly on the electron gyroradius for moderate potentials. For T_e=10 eV, the electron gyroradius increases, and therefore the collected currents for B_0=1 µT (squares) and B_0=5 µT (triangles) are found closer to the current in a unmagnetized medium.

3.3 Density-potential relation

The current-voltage characteristics obtained earlier enable to derive the relation between Φ_S and the various ambient parameters (N_e, T_e, B_0), providing the value of the photoemission production rate J_{ph0} is known. Figure 5 shows the resulting density-potential relation for J_{ph0}=50 µA m^{-2}. The unmagnetized curves are compared to the analytical solution for an unmagnetized point source, as obtained from Eq. (3) and (5) :

$$N_e\left(cm^{-3}\right) = \frac{A_S J_{ph0}}{0.026 A_T \sqrt{T_e}} \frac{1+\Phi_s/T_{ph}}{1+\Phi_s/T_e} \exp\left(-\Phi_s/T_{ph}\right) \qquad (6)$$

It is found that for B_0=0, $N_e(\Phi_s)$ is close to the analytical solution for a point source. This result is comprehensible as discussed earlier, because the complex geometrical ado not affect the current calculations. For T_e=1 eV, the effect of $\mathbf{B_0}$ is weak on $N_e(\Phi_s)$. This is due to the fact that both collected electron and ejected photoelectron currents are reduced under the effect of $\mathbf{B_0}$, but by the same order of magnitude, because T_{ph} is comparable to T_e in this case. This is not the case when T_e increases : plasma electrons become unmagnetized, while the emitted photoelectrons are already magnetized. Therefore, the influence of $\mathbf{B_0}$ becomes more significant in the resulting $N_e(\Phi_s)$ curves.

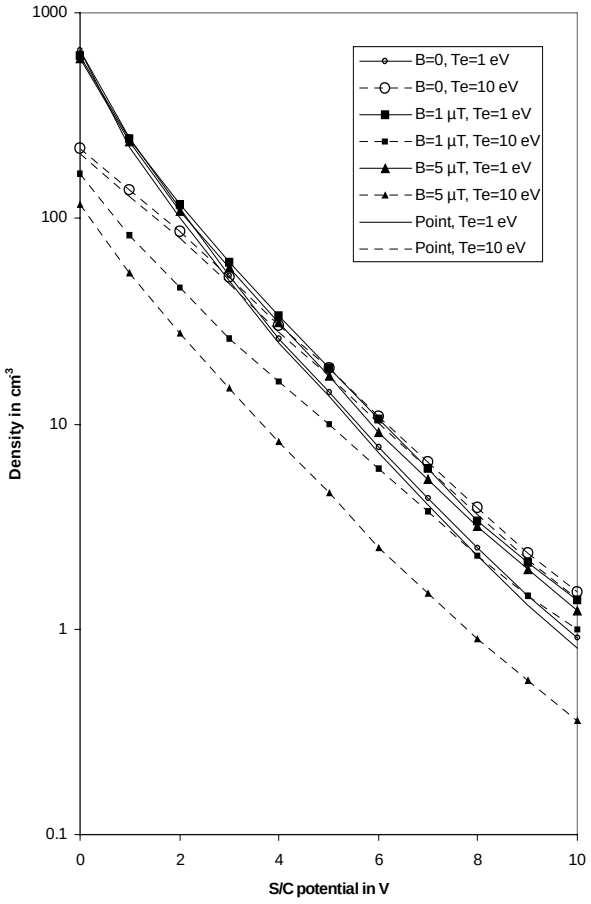

Figure 5. The plasma density as a function of the floating S/C potential for different values of T_e and B_0, as summarized in Table 1.

4. APPLICATIONS

4.1 Determination of the Photoemission rate

The aim of this section is to determine a value of J_{ph0} in the case of Interball AP. In this way, current-voltage characteristics from the simulations showed earlier, and data measurements aboard Interball-2 are used.

During several plasmapause crossings by Interball AP above 15000 km altitude, the S/C potential Φ_s and the plasma density N_e were measured simultaneously. The values of Φ_s were obtained from the electric-field double probe experiment, while N_e was determined from observations of the upper-hybrid resonance by the Polrad electric antenna.

Figure 6 shows the values of the S/C potential Φ_{sp} with respect to the probe and the electron density N_e during the period between July 1997 and October 1997. We found that with an average value J_{ph0}=35 µA m^{-2} and a temperature T_e=1 eV, the numerical $N_e(\Phi_{sp})$ relation reproduce perfectly well the measurements. The estimated value of J_{ph0} is very close to the value inferred from laboratory measurements (Ref. 4) which is about 30 µA m^{-2} for indium oxide surfaces.

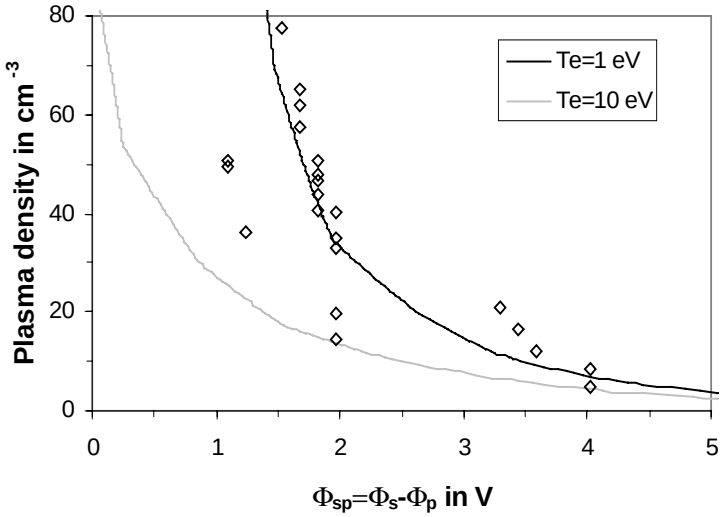

Figure 6. Results of diagnostic measurements: the diamonds show the measurements of N_e and Φ_{sp}. The $N_e(\Phi_{sp})$ curve was deduced from the $N_e(\Phi_s)$ relation for B_0=1 µT by estimating analytically the probe potential Φ_p with respect to the plasma.

4.2 Application to polar outflows

Figure 7 shows an example of polar cap crossing by Interball AP on August 8th 1997 between 5:00 and 6:00 UT. The first two panels show the presence of intense upflowing H^+ and O^+ ions, with a spin modulation about 2 min. Along Interball AP orbit, the S/C potential Φ_s was inferred from the electric field double-probe experiment. Therefore, it is possible to determine systematically the values of the plasma density N_e from the numerical relations, by taking a photoemission rate J_{ph0}=35 µA m^{-2}, And an electron temperature T_e=1 eV. In this region of the magnetosphere, the upflowing ions are the most dominant component, therefore their measurements can be used to determine the total plasma density. Unfortunately, due to the fact that a positive potential barrier is developed around the Hyperboloid instrument, a significant part of the thermal plasma is missed, and the ion density is subsequently underestimated by about 2 orders of magnitude, as shown in Figure 7. This problem is analyzed more quantitatively in another paper [10]. In this case, measurements of the S/C potential act as a useful diagnostic method to estimate the density of the polar ion outflows.

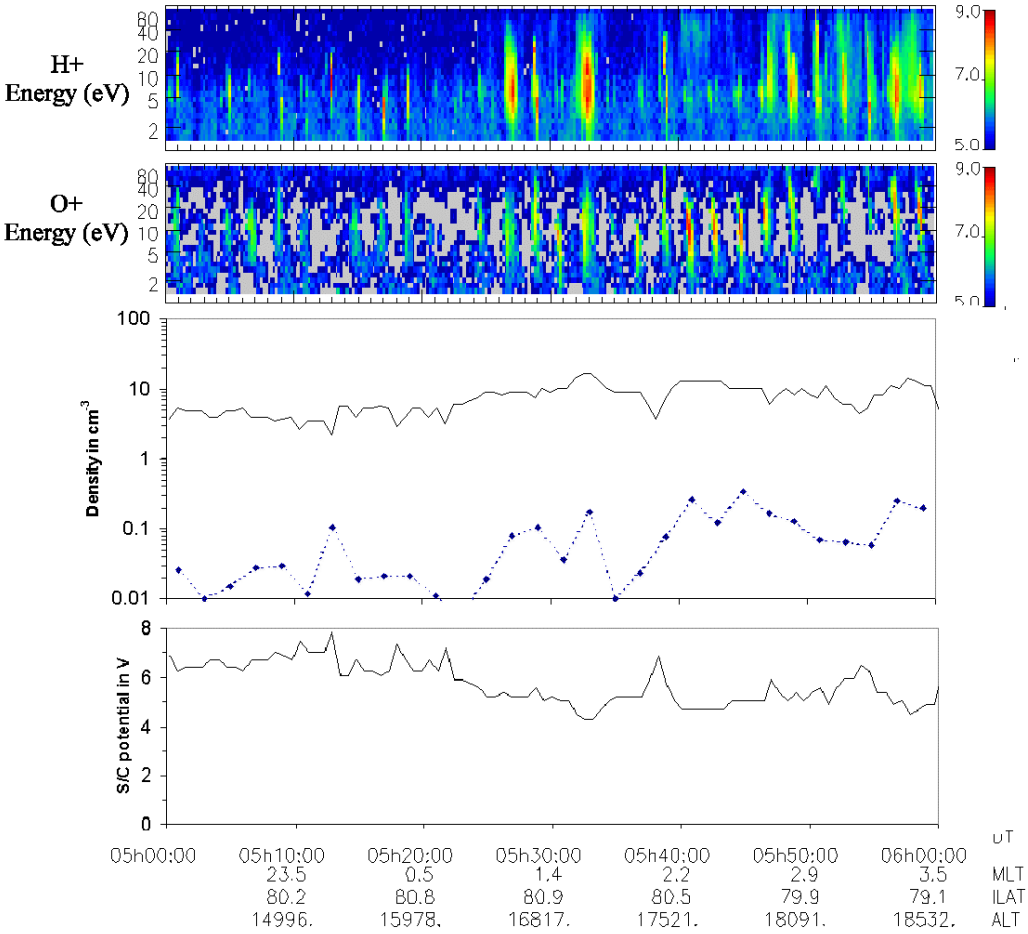

Figure 7. From top to bottom : Ion energy-time spectrograms of H^+ and O^+ ions recorded by the Hyperboloid experiment, calculations of the plasma density from numerical relations (solid) and from ion measurements (dot), and measurements of the S/C potential versus time.

5. CONCLUSION

A method for determining the floating spacecraft (S/C) potential of Interball AP as a function of the different ambient parameters (magnetic field, photoemission, electron density and temperature) is developed. The method used current-voltage relations of escaping photoelectrons and incoming plasma electrons, performed by modelling particle trajectories in a Laplace solution of the 3D potential structure around Interball AP. The main results are as follow :

- The effect of the complex geometry of Interball AP is weak for the determination of the potential
- In the case of a cold electron population (1 eV), the determination of the floating satellite potential is not sensitive to the value of the ambient magnetic field.
- In the case of more energetic electrons (10 eV), the determination of the floating satellite potential becomes sensitive to the value of the ambient magnetic field.
- The results were used to determine the photoemission production rate on the sunlit surface. A value of 35 $\mu A\ m^{-2}$ was estimated.

All these results are fundamental for correcting thermal plasma measurements, and particularly for the analysis of ion distributions measured by the Hyperboloid instrument.

References

1. Torkar, K., H. Jeszenski, M. V. Veselov, S. Perraut, N. Dubouloz, C.P. Escoubet, and Y. I. Galperin, Spacecraft potential measurements on board Interball-2 and derived plasma densities, *Cosmic. Res.*, 37, 606, 1999.

2. Dubouloz, N., J.-J. Berthelier, M. Malingre, L. Girard, Y. Galperin, J. Covinhes, D. Chugunin, M. Godefroy, G. Gogly, C. Guérin, J.-M. Illiano, P. Kossa, F. Leblanc, F. Legoff, T. Mularchik, J. Paris, W. Stzepourginski, F. Vivat, and L. Zinin, Thermal ion measurements on board Interball Auroral Probe by the Hyperboloid experiment, *Ann. Geophys.*, 16, 1070-1086, 1998.

3. Garrett, H.B., The charging of spacecraft surfaces, *Rev. Geophys. Space Phys.*, 19, 577-516, 1981.

4. Grard, R., Properties of the satellite photoelectron sheath derived from photoemission laboratory measurements, *J. Geophys. Res.*, 78, 2873, 1973.

5. Pedersen, A., Solar Wind and magnetosphere plasma diagnostics by spacecraft electrostatic potential measurements, *Ann. Geophys.*, 13, 118-129, 1995.

6. Escoubet, C.P., A. Pedersen, R. Schmidt, and P.A. Lindqvist, Density in the magnetosphere inferred from ISEE 1 spacecraft potential, *J. Geophys. Res.*, 102, 17595, 1997.

7. Zinin, L. V., Y. I. Galperin, V.A. Gladyshev, S.A. Grigoriev, L. Girard, and T.M. Mularchik, Modelling of the anisotropic thermal plasma measurements of the energy-mass-angle ion spectrometers onboard a charged satellite, *Cosmic Res.*, 33, 511, 1995.

8. Whipple, E. C., Theory of spherically symmetric photoelectron sheath: a thick sheath approximation and comparisons with the ATS 6 observation of a potential barrier, *J. Geophys. Res.*, 81, 601, 1976.

9. Bouhram, M., N. Dubouloz, and N. Singh, Sheath simulations for a high-altitude magnetospheric satellite: application to the Interball-2 case, *Geophys. Res. Lett.*, submitted, 2001.

10. Hamelin, M., et al., Combined effects of Hyperboloid outer geometry and potential bias on low energy ion measurements: corrected acceptance maps, this issue.